

Surface transport and anomalous bulk properties in topological insulator Bi_2Se_3

Yong Seung Kim^{1,2}, Matthew Brahlek¹, Namrata Bansal³, Eliav Edrey¹, Gary A. Kapilevich¹, Keiko Iida⁴, Makoto Tanimura⁴, Yoichi Horibe¹, Sang-Wook Cheong¹ and Seongshik Oh^{1,*}

¹ Department of Physics & Astronomy, The State University of New Jersey, Piscataway, New Jersey 08854, U.S.A.

² Department of Physics and Graphene Research Institute, Sejong University, Seoul 143-747 (Korea)

³ Department of Electrical and Computer Engineering, Rutgers, the State University of New Jersey, Piscataway, New Jersey 08854 (USA)

⁴ Research Department, Nissan Arc, Ltd., Yokosuka, Kanagawa 237-0061 (Japan)

* ohsean@physics.rutgers.edu

Abstract

We present two major breakthroughs in topological insulator (TI) transport properties. First, we demonstrate the existence of surface states in the transport channel of TI Bi_2Se_3 thin films, grown on Si with atomically-sharp interfaces. Second, we show that a number of transport properties in TI Bi_2Se_3 such as volume carrier densities, mobilities and surface magneto-conductance exhibit striking but well-

defined thickness-dependencies over as large as five orders of thickness (3 nm – 170 μ m). Understanding these anomalous bulk properties and their effects on the surface states seems to be a key step before TI applications can be envisioned.

Over the past few years, topological insulators (TI) have emerged as a new platform for coherent spin-polarized electronics. TIs are predicted to have an insulating bulk state and spin-momentum-locked metallic surface states [1-8]. This spin-momentum-locking mechanism and their band structure topology are predicted to prevent the surface metallic states from being localized due to backscattering. Among the TIs discovered so far, Bi_2Se_3 is considered the most promising due to its near-ideal surface-band structure [7]. Although the predicted surface states have been confirmed by a number of surface-sensitive probes on this material [5-6, 9-11], their signatures in transport properties have been very weak in bulk samples [11-14] and almost non-existent in thin films. The main problem behind this issue has been that the bulk states always turn out to be metallic instead of insulating, thus overwhelming the surface transport. This discrepancy between the theories and reality has put questions on many of the predictions, which are entirely based on the assumption of insulating bulk state. This Letter is the first exhaustive study of these metallic bulk states and their effects on the TI surface states, taken over many orders of sample thickness.

For this study, we grew Bi_2Se_3 films with atomically-sharp interfaces on Si(111) substrate by molecular beam epitaxy (MBE), covering more than three orders of thickness from 3 quintuple layers (QL, 1 QL \approx 1 nm) through 3,600 QL. From a technological point of view, silicon is the most important substrate for electronic applications. However,

interfaces between Bi_2Se_3 thin films and Si substrates have been plagued by disordered interfacial layers [14-15]. In order to solve this problem, we developed a two-step growth scheme and obtained high-quality second-phase-free Bi_2Se_3 films on Si substrates with atomically sharp interfaces; the growth details will be published elsewhere. Such an atomically-sharp interface is crucial for reliable thickness-dependent studies for very thin samples. A cross-section TEM image of a Bi_2Se_3 film in Fig. 1(a) shows an atomically sharp interface between the film and the Si substrate. The sharp reflection high energy electron diffraction (RHEED) pattern in the inset represents the high crystallinity of the Bi_2Se_3 film. Figure 1(b) shows X-ray diffraction (XRD) patterns for three different thicknesses. The peaks observed in the θ - 2θ scan are consistent with the c-axis oriented Bi_2Se_3 phase. During the growth of the film, the gap between each line in the RHEED pattern, which is inversely proportional to the in-plane lattice constant of the film, changed to that of the bulk lattice constant during the first QL growth. This immediate lattice relaxation is attributed to the weak van der Waals type bonding between the film and the substrate.

The transport measurements were carried out with the standard 4-point van der Pauw method in a cryostat with magnetic field up to 9 T and a base temperature of 1.5 K. For all films except for 3 QL, the R vs. T curves in Fig. 2(a) showed metallic behaviour at high temperature, but as the temperature dropped below 30 K the resistance tended to increase slightly either due to strong electron-electron interaction in the 2D limit [16] or due to an impurity band in the bulk [17]. The following measurements were all taken at a fixed temperature of 1.5 K.

It is well known that the mobility of conventional thin films depends on the film thickness as $\mu(t) = \mu_{\infty}/(1+2(\lambda/t)(1-p))$, where μ_{∞} is the mobility of the film when the thickness, t , is much larger than the mean free path, λ , with p representing the fraction of carriers reflecting specularly from the surface [18]; this mobility drop originates from the reduction in the effective mean free path caused by diffuse scattering from the surfaces. Figure 2(b) shows that the mobility vs. thickness data, obtained from Hall effect measurements, are in good agreement with this standard theory with $\mu_{\infty} \approx 3,000 \text{ cm}^2/\text{Vsec}$ and $\lambda(1-p) \approx 70 \text{ nm}$, except for the 3 QL data marked with a triangle. If the bulk of the film is insulating and the transport is entirely confined to the surfaces, the mobilities should be thickness-independent except for very thin samples where quantum tunnelling between the top and bottom surfaces can degrade the surface states [19-21]. The very observation of the conventional thickness-dependence implies that the observed mobilities are dominated by the bulk instead of the surface transport.

While the thickness-dependence of the mobilities can be well understood by the standard surface scattering theory, the thickness dependence of the volume and sheet carrier densities plotted in Figs. 2(c)-(d) is puzzling and unexpected. The volume carrier density (defined as the total sheet carrier density, obtained from the Hall measurement, divided by the sample thickness) decreases monotonically as the thickness increases and scales as $t^{-0.5}$ over three orders of thickness range, from $5.3 \times 10^{19} \text{ cm}^{-3}$ for 3 QL to $1.6 \times 10^{18} \text{ cm}^{-3}$ for 3,600 QL. Little change occurred in these values even after the films were annealed in high selenium vapour pressures, up to six orders of magnitude higher than the normal growth conditions; this implies that the observed carrier densities are close to the absolute

minimum values that are experimentally achievable in these pure Bi_2Se_3 films. We examined published data obtained from single crystal samples [17], and surprisingly these data points fall on the same curve, extending the trend up to five orders of thickness (3 nm - 170 μm) with $2 \times 10^{17} \text{ cm}^{-3}$ for 170 μm thick single crystal [17]. Considering that two completely different sample formation processes, one through MBE growth and the other through peeling of bulk samples [17], result in the same thickness-dependence suggests some fundamental mechanism behind this anomalous thickness-dependence of the carrier densities. Another view of this anomaly is through the thickness-dependence of the sheet carrier density. If we assume constant bulk volume carrier density (n_{bv}) and constant surface carrier density (n_{s}), the total sheet carrier density (n_{sheet}) should scale linearly with the sample thickness (t) such that $n_{\text{sheet}} = n_{\text{s}} + n_{\text{bv}}t$. In Fig. 2(d), the theoretical curve with $n_{\text{s}} = 2 \times 10^{13} \text{ cm}^{-2}$ and $n_{\text{bv}} = 1 \times 10^{18} \text{ cm}^{-3}$ was plotted for comparison with the experimental data. The observed data can in no way be explained by this simple model, and instead the total sheet carrier density scales as $t^{0.5}$. This is neither bulk nor surface alone, nor is it some linear combination with constant carrier density as the simple picture suggests. This implies that the bulk volume carrier density is not constant but varies monotonically with its thickness over five orders of magnitude. Considering that either the TI surface state [19] or the surface band-bending effect [22] can never extend more than tens of nanometers while the observed anomaly extends far beyond the micrometer scale, associating this observation with such an electronic mechanism seems unphysical. Because the volume carrier density mainly originates from the selenium vacancies [23], this observation nominally implies that the volume density of selenium vacancies gradually increases as samples get thinner. The formation of selenium vacancies through diffusion seems to

continuously occur even at room temperature, as confirmed by the observation that thin samples left in ultra high vacuum for an extended period exhibits an increased level of volume carrier densities. These observations suggest that formation of selenium vacancies in Bi_2Se_3 is thermodynamically favourable even at room temperature, yet it occurs through a slow diffusion process, which is inevitably thickness-dependent.

Although the surface states have not been clearly observed in the above two quantities, mobilities and carrier densities, due to the dominating bulk transport, magneto-resistance (MR) measurements presented below reveal clear signatures of the TI surface states. In Figs. 3(a)-(b), the MR, defined as $(R(B)-R(0))/R(0)$, in the high field regime is dominated by the parabola-like (B^2) dependence originating from the Lorentzian deflection of carriers under perpendicular magnetic field [24] (recall that the electron executes cyclotron orbits, thereby shortening the mean-free-path, and thus increasing the resistance). The fact that this B^2 -dependence is more pronounced in thicker samples suggests that it is a bulk-dominated effect.

In the low field regime (<0.5 T) for thinner samples, the magneto-conductance (MC), as shown in Fig. 4(a), decreases sharply as the magnetic field is increased, which is typical of the 2D weak anti-localization (WAL) effect [25-26]. This WAL effect is directly associated with the protection mechanism of the TI surface states, on which backscattering is at the minimum, when there is no magnetic field, due to the time-reversal symmetry. As magnetic field increases, thus breaking the time reversal symmetry, backscattering increases and leads to a sharp reduction in conductance. The low field MC, $\Delta G(B) = G(B) - G(0)$, can be well fitted to the standard Hikami-Larkin-Nagaoka (HLN) theory for WAL [27]: $\Delta G(B) = A(e^2/h)[\ln(B_\phi/B) - \Psi(1/2 + B_\phi/B)]$, where A is a coefficient predicted to be

$1/(2\pi)$ for each surface, B_ϕ is the de-phasing magnetic field, and $\Psi(x)$ is the digamma function. The de-phasing magnetic field is related to the phase coherence length l_ϕ via [16, 28] $B_\phi = \hbar/(4el_\phi^2)$. Figure 4b-c shows the fitting parameters as a function of thickness for 3-100 QL. The fitting parameter A remains approximately constant around $1/(2\pi)$ while the parameter l_ϕ monotonically increases as samples get thicker. The parameter A being closer to $1/(2\pi)$ than $1/\pi$ nominally implies that the top and bottom surfaces behave together like a single plane. However, considering the level of approximation in the HLN theory, its exact value may not have much physical meaning. Still, the parameter A being close to the predicted value over a wide thickness range implies that the WAL effect, which is one of the key mechanisms providing topological protection for the metallic surface states, is active in these Bi_2Se_3 thin films. Although the WAL signal became too small to be of quantitative relevance as the thickness increased beyond 100 QL, the spike in ΔG was still visible up to 3,600 QL as shown in the inset of Fig. 3(b), suggesting the robustness of the WAL effect. Below 5 QL, the WAL behaviour significantly degrades as the oppositely spin-polarized top and bottom surfaces start to couple strongly through quantum tunnelling [19-21].

Figure 4(c) shows that the parameter l_ϕ scales as $t^{0.7}$. In comparison, the mobility presented in Fig. 2(b) scales almost linearly with the thickness over the same thickness range (5 – 100 QL). If the bulk of the film is insulating, the phase coherence length, being a surface property, has to be independent of the thickness—the surfaces should not change when the thickness changes. However, with conducting bulk states, the top and bottom surfaces can interact with each other through the bulk, leading to a thickness-dependent

scattering mechanism. In other words, the thickness-dependent coherence length shown in Fig. 4(c) is a natural result of the metallic bulk states. In addition to the inter-surface scattering, the increase in volume carrier density as observed in Fig. 2(c) will also result in a rise in surface-bulk scattering events, leading to a reduced coherence length as films get thinner. However, the fact that the thickness-dependence of the phase coherence length is weaker than that of the mobility does confirm that the WAL signal is dominated by the surface states, even with significant bulk carriers around. This dimensional selectivity of the WAL signal also explains why we could clearly resolve the surface states with the WAL effect even though the mobilities and carrier densities obtained from Hall measurements, which are dimensionally non-selective, failed to provide any signatures of the surface transport.

In summary, all the measured bulk and surface transport properties showed striking thickness dependencies over a wide thickness range. In particular, the volume carrier density, which is commonly assumed to be thickness-independent, decreased by more than two orders of magnitude over the thickness of five orders. The thickness dependence of the WAL effect suggests that the metallic bulk state allows the top and bottom surface carriers to interact with each other. So far theoretical studies of TIs have almost entirely assumed the ideal, insulating bulk state, although all existing TIs exhibit metallic bulk properties. Our observations suggest that these metallic bulk states entail a number of unexpected behaviours not only for the bulk but also for the surface states. New theoretical approaches taking into account the metallic bulk states and their interactions with the surface states will be necessary to properly describe real TIs.

We thank Keun Hyuk Ahn for reviewing the manuscript before submission. This work is supported by IAMDN of Rutgers University, National Science Foundation (NSF DMR-0845464) and Office of Naval Research (ONR N000140910749).

References

- [1] M. Z. Hasan, C. L. Kane, Rev. Mod. Phys. **82**, 3045 (2010).
- [2] X. L. Qi, S. C. Zhang, Phys. Today **63**(1), 33 (2010).
- [3] J. E. Moore, Nature **464**, 194 (2010).
- [4] D. Hsieh *et al.*, Nature **460**, 1101 (2009).
- [5] H. L. Peng *et al.*, Nat. Mat. **9**, 225 (2010).
- [6] Y. Xia *et al.*, Nat. Phys. **5**, 398 (2009).
- [7] H. J. Zhang *et al.*, Nat. Phys. **5**, 438 (2009).
- [8] Y. L. Chen *et al.*, Science **325**, 178 (2009).
- [9] T. Hanaguri, K. Igarashi, M. Kawamura, H. Takagi, T. Sasagawa, Phys. Rev. B **82**, 081305 (2010).
- [10] P. Cheng *et al.*, Phys. Rev. Lett. **105**, 076801 (2010).
- [11] J. G. Analytis *et al.*, Nat. Phys. **6**, 960 (2010).
- [12] N. P. Butch *et al.*, Phys Rev B **81**, 241301 (2010).
- [13] A. Richardella *et al.*, App. Phys. Lett. **97**, 262104 (2010).
- [14] H. D. Li *et al.*, New J. Phys. **12**, 103038 (2010).
- [15] G. H. Zhang *et al.*, App. Phys. Lett. **95**, 053114 (2009).
- [16] M. Liu *et al.*, arXiv, 1011.1055 (2010).
- [17] J. G. Analytis *et al.*, Phys. Rev. B **81**, 205407 (2010).
- [18] A. Elshabini, F. D. Barlow, Thin film technology handbook. (McGraw-Hill, New York, 1998).
- [19] J. Linder, T. Yokoyama, A. Sudbø, Phys. Rev. B **80**, 205401 (2009).
- [20] Y. Zhang *et al.*, Nat. Phys. **6**, 584 (2010).

- [21] H.-Z. Lu, W.-Y. Shan, W. Yao, Q. Niu, S.-Q. Shen, Phys Rev B **81**, 115407 (2010).
- [22] M. Bianchi *et al.*, Nat. Commun. **1**, 128 (2010).
- [23] Y. S. Hor *et al.*, Phys. Rev. B **79**, 195208 (2009).
- [24] J. M. Ziman, Electrons and phonons; the theory of transport phenomena in solids.
(Clarendon Press, Oxford, 1960).
- [25] J. Chen *et al.*, Phys. Rev. Lett. **105**, 176602 (2010).
- [26] J. G. Checkelsky, Y. S. Hor, R. J. Cava, N. P. Ong, arXiv, 1003.3883 (2010).
- [27] S. Hikami, A. Larkin, Y. Nagaoka, Prog. Theor. Phys. **63**, 707 (1980).
- [28] H.-T. He *et al.*, arXiv, 1008.0141 (2010).

Figure Legends

FIG. 1 (color online). Epitaxial growth of Bi_2Se_3 film.

(a) Cross-section TEM image of 32 QL film shows atomically sharp interface between Bi_2Se_3 and a Si substrate. Inset: RHEED pattern of the Bi_2Se_3 film. (b) High-resolution X-ray diffraction pattern of three different films.

FIG. 2 (color online). Thickness dependence of the transport properties of Bi_2Se_3 .

(a) Resistance of Bi_2Se_3 films as a function of temperature with thickness ranging from 3 to 3,600 QL. Data above ~ 150 K are not shown here because they are affected by the parallel conduction from thermally excited carriers in the un-doped silicon substrates. (b) Mobility, (c), (d) Carrier density of electrons in Bi_2Se_3 films obtained by Hall measurement at 1.5 K. The solid curve in (b) is $\mu(t) = 3,000/(1+140/t)$, and the straight lines in (c) and (d) are illustrative guides.

FIG. 3 (color online). Normalized Magnetoresistance.

The magnetic field dependence of resistance at 1.5 K of (a), thin film from 3 to 32QL and (b) thick film from 60 to 3,600 QL. Deep cusp in low field regime is characteristic of the WAL effect. Parabolic field dependence is dominant in thick films. Inset of (b): zoomed-in view of the 3,600 QL data near zero field showing robustness of the WAL effect.

FIG. 4 (color online). Weak anti-localization effect.

(a) The HLN fitting of the change in conductance in low field regime from 3 to 100 QL. (b) Above 5 QL, the coefficient A is almost thickness-independent and consistent with the

predicted value in the 2D WAL regime. (c) The phase coherence length increases as $t^{0.7}$ with the sample thickness.

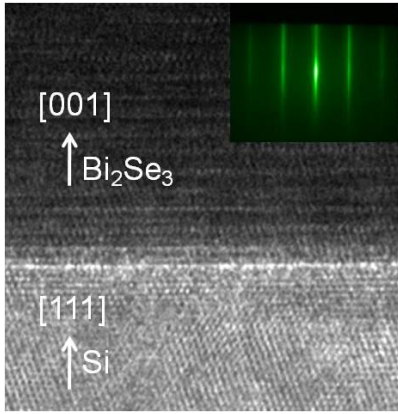


Fig. 1(a)

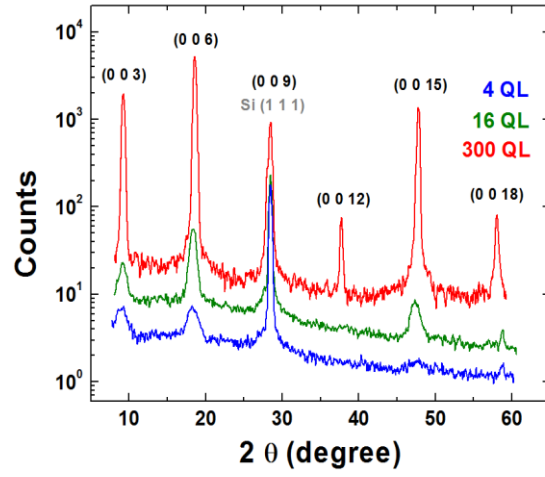


Fig. 1(b)

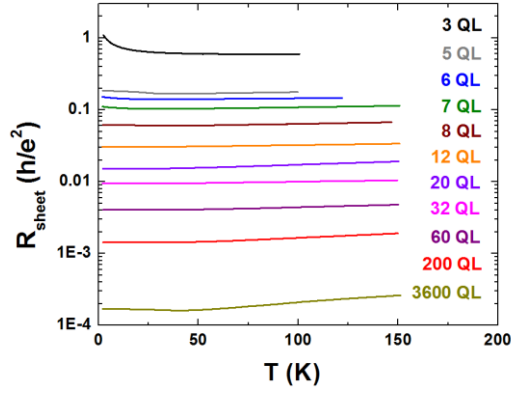


Fig. 2(a)

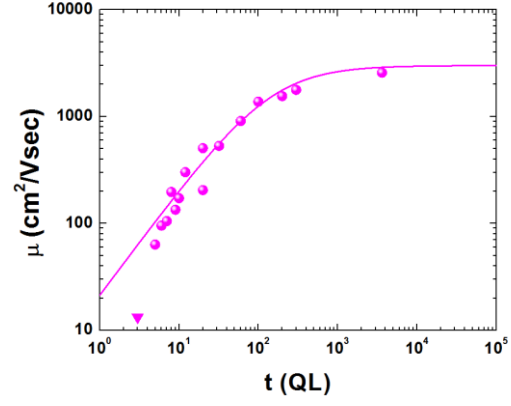


Fig. 2(b)

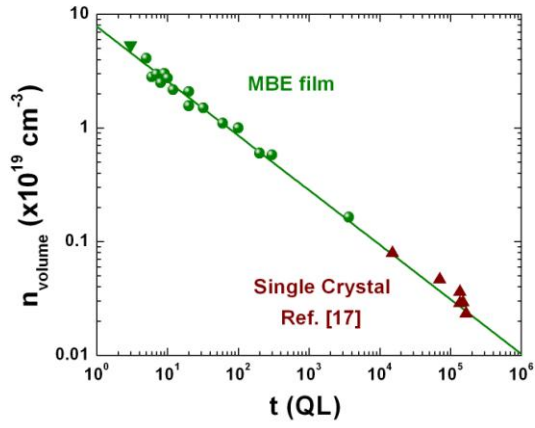


Fig. 2(c)

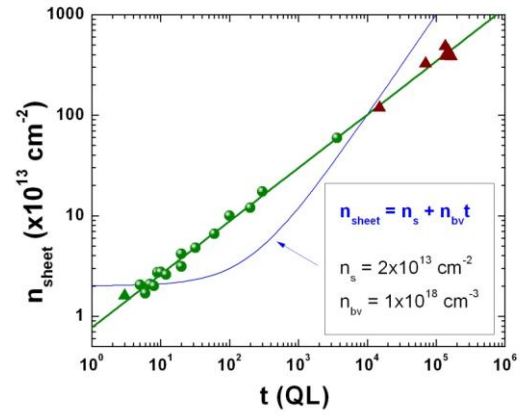


Fig. 2(d)

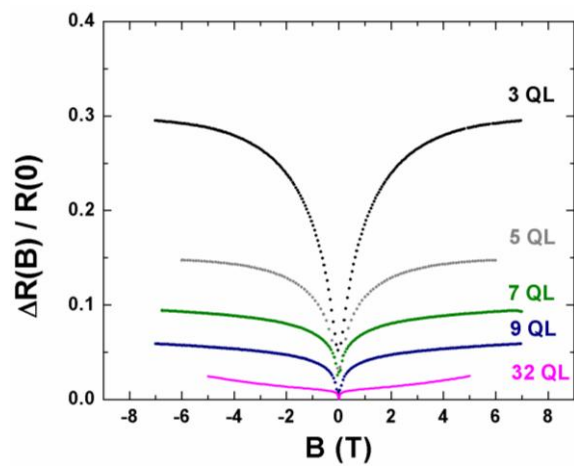


Fig. 3(a)

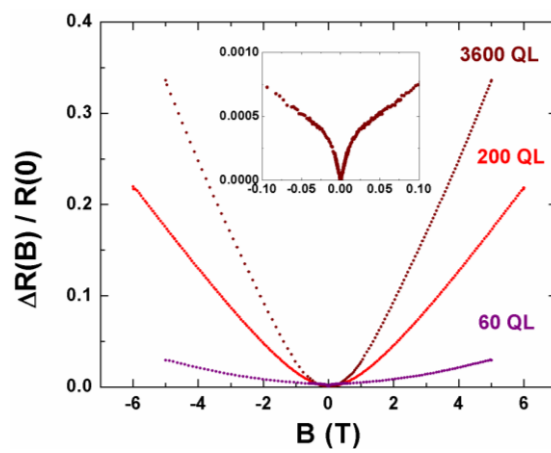


Fig. 3(b)

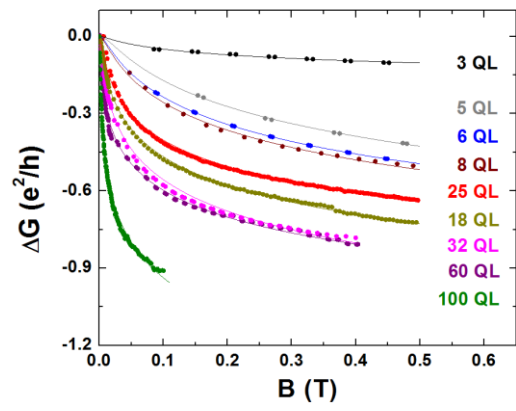


Fig. 4(a)

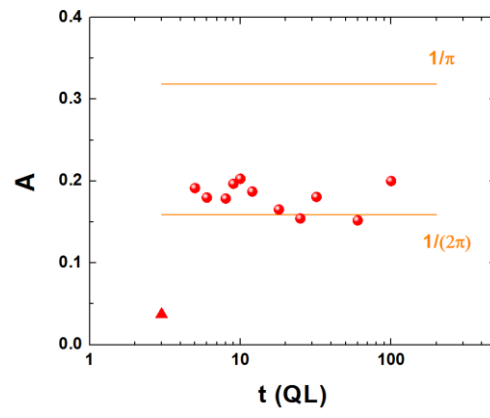


Fig. 4(b)

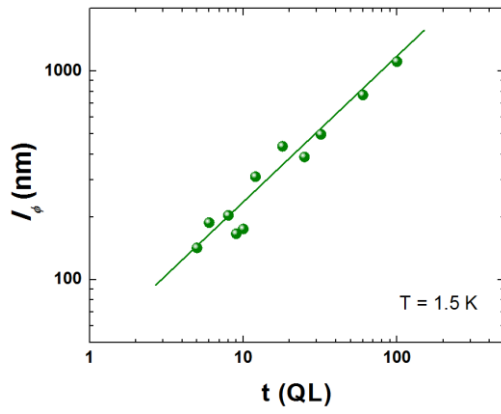


Fig. 4(c)